Observations and improvements on the impact-echo method used for blast furnace hearth refractory measurement

Commandeur, C.; Sprik, R.; Stolk, C.; Louwerse, G.

DOI
10.1080/03019233.2022.2081956

Publication date
2023

Document Version
Final published version

Published in
Ironmaking and Steelmaking

IRONMAKING & STEELMAKING
2023, VOL. 50, NO. 1, 30–43
https://doi.org/10.1080/03019233.2022.2081956

I·M3 Institute of Materials, Minerals & Mining
Taylor & Francis
Taylor & Francis Group

RESEARCH ARTICLE

Observations and improvements on the impact-echo method used for blast furnace hearth refractory measurement

Colin Commandeur[a], Rudolf Sprik [b], Chris Stolk [c] and Gerard Louwerse[a]

[a]Tata Steel, IJmuiden, Netherlands; [b]Van der Waals-Zeeman Institute, University of Amsterdam, Amsterdam, Netherlands; [c]Korteweg-de Vries Institute, University of Amsterdam, Amsterdam, Netherlands

ABSTRACT
The refractory thickness of the blast furnace hearth is a critical parameter for the safe operation of a blast furnace. A replacement of the refractory comes with high costs and, therefore, unnecessary repairs should be avoided. A promising method to estimate the refractory thickness is the impact-echo method. For the interpretation of impact-echo, often, the peaks in the spectrum of the measured signal are associated with the echo from an interface. In this paper, it is shown that this method should be used with care when applied to multi-layered structures. An alternative approach is presented for the calculation of the thickness of multi-layered structures. This method solves the wave equation based on transmission line theory. The formula is checked against 2D finite element analysis and for simple layered structures, good agreement is found. Three cases are simulated using finite element models. Both the impact-echo method and the proposed method overestimate the refractory thickness.

ARTICLE HISTORY
Received 31 March 2022
Accepted 20 May 2022

KEYWORDS
Blast furnace hearth; impact-echo; refractory; FEM; Hearth monitoring; Inverse modelling; Acoustic measurements; Hearth erosion

Introduction

The refractory in the hearth of the blast furnace will erode due to mechanical, chemical and thermal wear. A breakout of the hearth wall will cause danger and damage and is a very costly event. To safely run a blast furnace at high production rates, it must be sure that the walls are able to withstand the liquid metal.

Traditionally thermocouple measurements are used for the estimation of refractory thickness. The downside of using thermocouples is that they must be installed at fixed locations. At each of these locations, a hole needs to be drilled in the blast furnace shell and refractory for installing the thermocouple. In this paper, the use of the impact-echo method is explored for measuring refractory thickness.

Impact-echo has been used extensively in the civil industry for measuring the integrity of concrete slabs. In this method, an acoustic pulse is launched by the use of an impactor, and the echoes of the pulse are received by a receiver. The received pulses are processed to yield the thickness of the object under test. For the interpretation of the results often, a formula is used, which is based on the travel time of the excited pulse. The travel time is used to calculate the frequency by which the pulse travels back-and-forth to the corresponding interface. This approach works well for the thickness measurement of a single layer. In this work, a more general approach is proposed, which includes the thickness estimation of multi-layered structures. This method solves the scalar acoustic wave equation by using an acoustic transmission line method (TLM).

The proposed formula is tested using a 2D finite element approach and produces good results where the method based on pulse travel time fails. A method based on travel time would predict fixed frequency positions for each interface encountered by the acoustic wave. For example, in the presence of a skull layer, it will predict an additional peak in the spectrum below the peak that is related to the refractory thickness, while the peak related to the skull-refractory interface remains at the same frequency. Both the 2D FEM and transmission line approach show that the peak related to the refractory thickness will be shifted. This may pose a serious issue for the interpretation of field measurements if a method is used that is based on the inversion of a single frequency.

Three cases are discussed in which the performance of the 1D approach is examined using a 2D axisymmetric finite element simulation. When testing the 1D approaches using more realistic blast furnace geometries in 2D axisymmetry large errors may occur. The spectra in these cases have a multitude of peaks, and it is non-trivial to select a peak to use in the 1D inverse model.

The findings from the cases are still optimistic as many real-world factors have been left out of the simulation, e.g. interfaces are still assumed to have perfect contact, the seams between bricks of the same material are neglected, and no thermocouples are present in the refractory, the bricks are assumed to be isotropic. This means that in practice the errors may even be bigger.

The point of impact behaves like a points source as the wavelengths involved are much larger than the impactor size. The wave created by impact-echo propagates in all directions throughout the shell and refractory. Therefore, the pulse will not propagate in a straight line back-and-forth from the refractory-skull interface. The pulse reflects a large array on the refractory-skull interface rather than a small point at the same height as the point of impact. It can be expected that a simple one-dimensional approach will lead to inaccurate results.

In this work, three cases have been investigated where the 1D approach is applied to the results of a 2D axisymmetric

CONTACT Colin Commandeur colin.commandeur@tatasteeleurope.com 1970 CA Velsen-Noord

finite element simulation. The thickness was, in some cases, overestimated by more than 26%.

To control the wear of refractory the furnace is cooled sufficiently to freeze some of the liquid metal onto the refractory. This layer of solidified material is called the skull layer. In the last paragraphs, the influence of the skull layer is discussed. The presence of a skull layer can have a large effect on the measurement. In the final section, it is argued that an inversion method based on temperatures may yield better accuracy than non-destructive acoustical methods.

The impact-echo method

The impact-echo method was developed by Sansalone and Carino [1]. The use of an impactor makes it very practical to introduce sufficient energy in the test object without having to do a careful preparation of the surface. The use of a broadband accelerometer coupled by a lead strip instead of coupling gels makes the method very suitable to apply in the field on concrete structures, which are hard to measure using ultrasonic methods. In the book by Sansalone and Streett [2], the impact-echo formula is presented for single-layered structure:

$$f = \frac{\beta V}{2T} \tag{1}$$

In which β is the shape factor which is used to account for the shape of the object. Empirically the shape factor was found to be 0.96. In later work, the shape factor could also be explained theoretically by using Lamb wave theory [3]. The observed frequency was found to coincide with the zero phase group velocity (ZGV) of the first symmetric mode (S_1). The shape factor is found to be slightly dependent on the Poisson's ratio of the materials under test.

Also it was recognized that if the plate is backed by a material with a high acoustic impedance, the wave will not reflect as a tension wave but as a compression wave. In this case, the frequency at which the wave constructively interferes with itself is halved with respect to Equation (1).

In the same book by Sansalone, a formula is presented to extend Equation (1) to multiple layers. For the derivation, it is argued that when a pulse travels through a multi-layered medium, the pulse may change phase when transmitted through an interface, but this phase change will be undone when the wave is traveling back towards the source. The formula basically calculated the travel time of the wave to travel to and from the interface. The accompanying frequency is considered the reciprocal of the total travel time. In Figure 1, a simple layered structure is depicted on the right side the steps in derivation of Equation (2) are shown.

$$f = \frac{1}{\frac{2T_1}{\beta_1 V_{p1}} + \frac{2T_2}{\beta_2 V_{p2}} + \dots} \tag{2}$$

As this can be thought of as the pulse repetition frequency the formula will be referred to as PRF method in the remainder of the text.

The PRF method does not sum the reflections from the intermediate interfaces and multiples of these reflections. Hence, it does not account for the interference of the wave with itself. It also does not account for the variation of different boundary conditions. If the pulse travel time is calculated it is not relevant if the pulse is inverted upon reflection or not. However, at low frequencies where interference of the wave with itself needs to be taken into account, it does matter if the phase of the pulse changes upon reflection, as was the case for a single layer with either a soft or hard backing material.

It is demonstrated in [2] that, to achieve good results with this method for multi-layer media, the material parameters such as the longitudinal wave speed have to be adapted. This approach can be successful when the method is used for anomaly detection. In this case, the reference spectrum can be measured on a test piece, in the cases where the field measurements deviate too much from the reference, the location can be marked.

The impact-echo method started to be used for the estimation of the wall thickness of blast furnaces [1]. However, there are several important differences with concrete slabs which make the application of impact-echo for this purpose much more challenging:

- A concrete slab has a relatively small thickness in the direction of measurement and a much larger dimension in the lateral directions.
- In civil applications, the geometry of the healthy structure is often known *a priori*. In the case of the blast furnace, the geometry of the structure is to be estimated.
- The concrete slab can be accessed directly, whereas a blast furnace has a thick steel shell on the outside. This layer is often several centimeters thick, and the acoustic impedance is quite different from the furnace refractory.
- During the operation of the furnace, a large temperature gradient is present, which alters the material properties.

From a physics perspective, the PRF method neglects interference effects and, therefore, this interpretation is only valid when limited interference with the reflected signals is taking place. One can think of situations where the pulse lengths are very small compared to the thickness of the slabs. However, in these cases, an analysis in the time domain would make more sense, as is done in the ultrasonic pulse-echo method.

The wave speed in the steel shell is around 5800 m s^{-1}, at a frequency of 5 kHz, the wavelength will be 1.16 m, which is much longer than the thickness of the shell. A pulse length of 5 mm would require 1.16 MHz. This indicates that interference effects should be taken into account. The pulse created by the hammer will create a complex interference pattern within the refractory.

By using a hammer for excitation of the acoustic pulse, a broad spectrum is excited. To have sufficient energy in the frequency of interest the contact time needs to be sufficiently long. In Ref. [2], the maximum usable frequency, f_{max}, is related to the contact time, t_c, as $f_{max} = 1.25/t_c$. If the maximum useable frequency is about 5 kHz. The contact time is 250 µs, implying that during this time, the wave has travelled about 1.45 m in the steel layer. In other words, the pulse has already travelled 24 times up and down the shell-refractory interface. This indicates that no isolated pulses are produced.

Rather than introducing isolated pulses, one excites a broad spectrum of frequencies which interfere either constructively or destructively. The destructively interfering frequencies die out more quickly than the constructively

interfering frequencies. The frequencies that survive may be regarded as the eigenmodes of the structure under test. The return signal is a summation of the eigenmodes; it both depends on the position of the impact and the position of the receiver in which extent each eigenmode is excited and measured.

Transmission line method

As an alternative to the pulse repetition frequency formula one may solve the scalar acoustic wave equation. In this approach the analogy with electrical transmission lines is exploited. This approach is also described by Pollard [4].

If we consider the simple wave eigenvalue problem known as the Helmholtz equation shown in Equation (3).

$$\nabla \cdot \frac{1}{\rho} \nabla P = -\frac{\omega^2}{\rho c^2} P \tag{3}$$

where ω is the radial frequency, ρ is the material density and c is the wave speed. Both the density and wave speed vary with position as these parameters are different in the different materials used and are also dependent on temperature. In this work, the density is considered constant in each domain. However, the density is allowed to jump at the interfaces.

For a one-dimensional model, only a single dimension is considered, and the formula, in this case, simplifies to Equation (4).

$$\partial_x \frac{1}{\rho} \partial_x p = -\frac{\omega^2}{\rho c^2} p \tag{4}$$

At interfaces, we require a continuity of pressure and flux and, therefore, at internal boundaries, we require the satisfaction of Equation (5).

$$\begin{aligned} p_i &= p_j \\ \rho_i \partial_x p_i &= \rho_j \partial_x p_j \end{aligned} \tag{5}$$

The subscripts i and j indicate the domain numbers at each side of the interface. In many cases, the density is considered constant for which case the density drops out of the equation. In our case, the density is an important parameter that will determine the phase and the amplitude of the reflected signals.

The pressure at the excitation location is given by the excess pressure due to the input force. The excess pressure after the excitation is zero and therefore implies a free boundary condition.

The measurand is the acceleration at this location and is calculated from Equation (6).

$$a = -\frac{1}{\rho} \partial_x p \tag{6}$$

Table 1. Material properties.

Material	Density [kg/m^3]	Young's modulus [GPa]	Poisson ratio	*P*-wave velocity [m/s]	S-wave velocity [m/s]
Shell	7800	203	0.285	5803	3182
Graphite	1750	6.0	0.200	1952	1195
Ramming	1500	3.2	0.272	1636	916
Semi-graphite	2500	14.4	0.272	2689	1505
Skull	7290	126	0.285	4729	2358

A practical way to solve this system of equations in 1D a transmission line approach is suggested. This approach is described in [5]. Each layer may be described by an acoustic transmission line. The transfer matrix is described by Equation (7).

$$\begin{bmatrix} p_1 \\ v_1 \end{bmatrix} = \begin{bmatrix} \cosh(\gamma l) & Z_0 \cdot sinh(\gamma l) \\ \frac{1}{Z_0} sinh(\gamma l) & \cosh(\gamma l) \end{bmatrix} \begin{bmatrix} p_2 \\ v_2 \end{bmatrix}$$

The output vector contains the pressure p_1 and velocity v_1 at the front side of the layer and the input vector contains the pressure p_2 and velocity v_2 at the backside of the layer. This matrix can be cascaded for the calculation of a system composed of multiple layers. Notice that in this approach, we can account for the type of backing material. A propagation constant is a complex number in general. If damping is neglected, the matrix can be simplified by using the identities $sinh(x) = -i \cdot sin(ix)$ and $cosh(x) = cos(ix)$. The imaginary part of the propagation constant is equal to the angular phase constant, k.

$$\begin{bmatrix} p_1 \\ v_1 \end{bmatrix} = \begin{bmatrix} \cos(kl) & jZ_0 \cdot sin(kl) \\ \frac{j}{Z_0} sin(kl) & \cos(kl) \end{bmatrix} \begin{bmatrix} p_2 \\ v_2 \end{bmatrix} \tag{8}$$

It is possible to consider different boundary conditions for the type of backing of the last layer. If an acoustically light material is used a soft boundary condition can be applied by setting the external pressure p_2 to zero. The acoustic impedance, Z, of a material relates to the ratio of pressure and particle velocity, or $Z = p_1/v_1$. The acoustic impedance of a single layer with a free boundary condition can thus be calculated using Equation (9).

$$\begin{aligned} \begin{bmatrix} p_1 \\ v_1 \end{bmatrix} &= \begin{bmatrix} \cos(kl) & jZ_0 \cdot sin(kl) \\ \frac{j}{Z_0} sin(kl) & \cos(kl) \end{bmatrix} \begin{bmatrix} 0 \\ v_2 \end{bmatrix} \\ &= \begin{bmatrix} jZ_0 \cdot sin(kl) \\ \cos(kl) \end{bmatrix} v_2 \end{aligned} \tag{9}$$

$$Z_1 = \frac{p_1}{v_1} = j Z_0 \, tan(kl) \tag{10}$$

In impact-echo, we use a force to excite the wave, and the acceleration is measured. Therefore resonance peaks are measured at the frequency where the impedance goes to zero. This is the case when the argument of the tangent is π, or where the thickness is a half wavelength or a multiple of this. The first resonance frequency is correctly predicted by the original impact-echo formula as well.

For a hard backing material it is found that resonance occurs at a quarter of the wavelength plus multiples of half a wavelength.

Solutions for a composite layer of two layers can also be found from Equation (11) as published in [5]:

$$\rho_1 c_1 tan\left(\frac{2\pi f_c T_1}{c_1}\right) + \rho_2 c_2 tan\left(\frac{2\pi f_c T_2}{c_2}\right) = 0 \tag{11}$$

If Equation (2) is correct, it will provide an easy way to estimate the resonance frequency. However, it can be found from inspection that Equation (2) does not provide a general solution to this problem. With the TLM approach Equation (11) is easily derived from multiplying the two transfer matrices of both layers, applying an open boundary condition and setting the resulting impedance to zero.

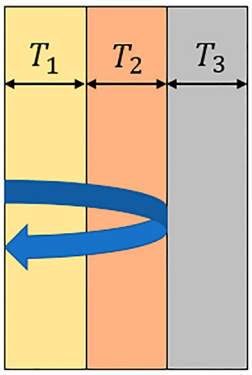

$$t_i = \frac{T_i}{\beta_i V_{p,i}}$$

$$t_{2-3} = 2t_1 + 2t_2$$

$$f_{2-3} = \frac{1}{t_{2-3}}$$

Figure 1. The frequency associated with the interface between layer 2 and 3 is associated with the reciprocal of the travel time back and from this interface.

In the following, the effect of temperature on the material properties is neglected. However, if desired, it is possible to approximate temperature gradients by dividing the material into small parts and set the local properties according to the local temperature.

Elastic wave equation

In the next chapter, the 1D approach is tested by solving the elastic wave equation in a 2D axisymmetric context. The formulae in the previous paragraphs neglect any shear forces in the medium. A wave travelling in a solid material supports both compression waves as well as shear waves. The 1D formulae do not consider the presence of shear waves but should produce correct results for the spectrum produced by the longitudinal waves.

For the 2D simulations, the Navier equation is expressed as:

$$\rho \partial_{tt} d - \nabla \cdot \tau = f \tag{12}$$

Where the stress tensor, τ, is expressed using the Lamé parameters

$$\tau = 2\mu\varepsilon + \lambda \nabla \cdot d\, I, \qquad \varepsilon = 0.5(\nabla d + (\nabla d)^T) \tag{13}$$

The Lamé parameters for the plane strain conditions where $\varepsilon_{zz} = \varepsilon_{xz} = \varepsilon_{yz} = 0$ are given in Equation (14).

$$\lambda = \frac{E}{(1+\nu)(1-2\nu)}, \qquad \mu = \frac{E}{2(1+\nu)} \tag{14}$$

In the absorbing boundaries of the problem, the Rayleigh damping is applied.

The equations are solved by using Elmer FEM, an open-source code for simulating multi-physics problems [6].

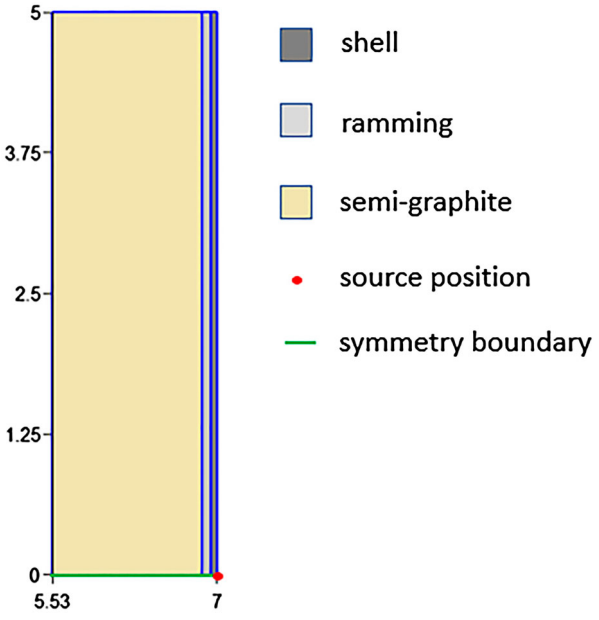

Figure 2. Geometry for a simple layered model. A symmetry boundary is applied at the bottom. The material properties used for each layer are found in Table 1.

Comparison with 2D finite element computations

The 1D approach is tested here against 2D finite element analysis. By solving the elastic wave equation in two dimensions, it is possible to assess the performance of the 1D equation in a 2D setting.

To make the comparison more interesting in relation to the application of the method on a blast furnace hearth, a similar layer setup is considered. A 6 cm layer represents the shell and material properties similar to that of steel are applied. The shell layer is followed by an 8 cm ramming layer and 1.33-m thick semi-graphite layer. The backside is considered to be a free boundary condition where the pressure is zero. An absorption layer is applied to simulate infinite extent towards the top and bottom. The geometry used for the analysis is shown in Figure (2).

The 2D modelling is done in Elmer FEM [6], which is used to solve a time transient elastic wave equation using axisymmetry. For the excitation pulse, a Ricker wavelet is used with a central frequency of 2 kHz. As shown later, the frequencies that we are looking for are around 1 kHz. An interesting property of the TLM method is that also the higher harmonics can be predicted. This is advantageous as higher frequencies will result in a higher spatial resolution when the wavelengths become shorter.

For the calculations in this paper, the material properties shown in Table 1 are used

In Figure 3 the results of the calculations are shown. The horizontal displacement is extracted from the finite element solution. A spectrum is calculated using a Fourier transform of the signal after the initial pulse has finished. The curve marked with asterisks plots the spectrum calculated on a Cartesian geometry. In addition, a 2D FEM calculation is done for the axisymmetric case. In this case, an outer radius of 7 m is considered; the result for this case is shown as the curve marked with open circles in Figure 3. These two curves are quite similar. The first peak in the spectrum at 833 Hz is slightly shifted upwards to 842 Hz due to the axisymmetry. The effect is small as the radius is fairly big.

The dashed vertical lines indicate the frequencies calculated by solving the 1D scalar wave equations using the TLM model. The dash-dot vertical line shows the position of the peak as predicted by the PRF method.

From the figure, it is found that the 1D model predicts peaks at 833, 1539, 2277 and 3165 Hz. The PRF method predicts a frequency of 869 Hz. The first frequency is predicted well by the TLM method, but the higher frequencies are slightly lower than the result from the FEM model. The PRF

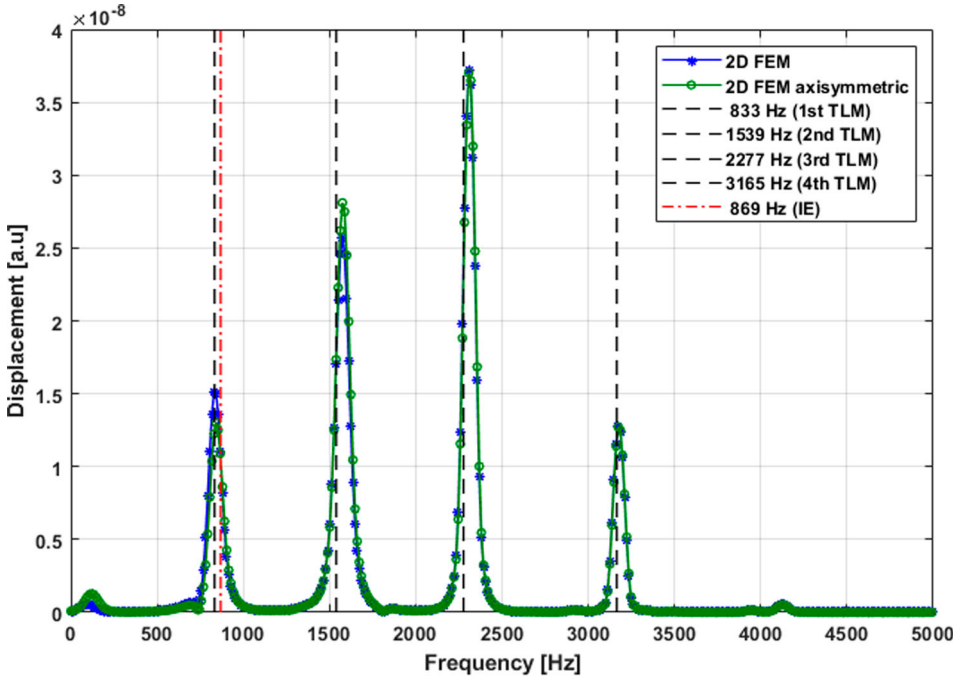

Figure 3. Response using square geometry with absorbing top and bottom boundary. Layer setup consisting of 6 cm shell, 8 cm ramming and 1.33 m semi-graphite. The curve marked with asterisks is the result from 2D finite element modelling of the planar geometry, the curve marked with open circles is simulated by assuming axisymmetry.

method predicts a slightly higher frequency (36 Hz) for the first peak.

In Figure 4, two curves are shown. The curves are calculated by the 1D models by starting at a total thickness of 2.2 m and iteratively shortening the semi-graphite stone. For the TLM model, the lowest peak in the spectrum is chosen. From the graph, we find that the difference between the two curves gets smaller as the wall gets thicker. At the first point, a total thickness of 0.2 m, the frequency predicted by the TLM model is about half of the PRF model. Another clear effect is that the slope of the curve flattens at higher thickness. This means that a small error in the frequency can lead to a high error in the estimated thickness.

From Figure 4, it is clear that the two models will show a larger difference when the wall becomes thinner. This is tested by adapting the semi-graphite thickness in the FEM model to 0.4 m. The result of this calculation is shown in Figure 5. There is a very good match between the predicted peak by the transmission line model. The TLM model predicts a resonance at 1618 Hz. The PRF model predicts a peak at 2323 Hz. In this case, the impact-echo model is clearly predicting the position of the peak not very well.

A more difficult issue is the presence of a welladhered skull. The PRF model would predict an additional second peak which is at a lower frequency with respect to the peaks that are predicted in the absence of the skull [7]. The

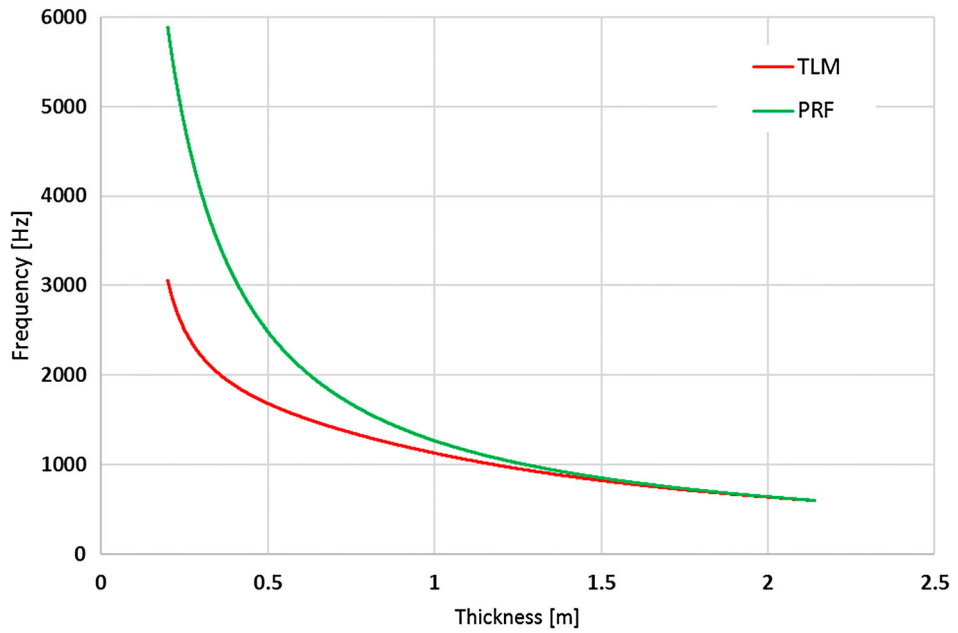

Figure 4. Thickness versus dominant frequency for the impact-echo and TLM models.

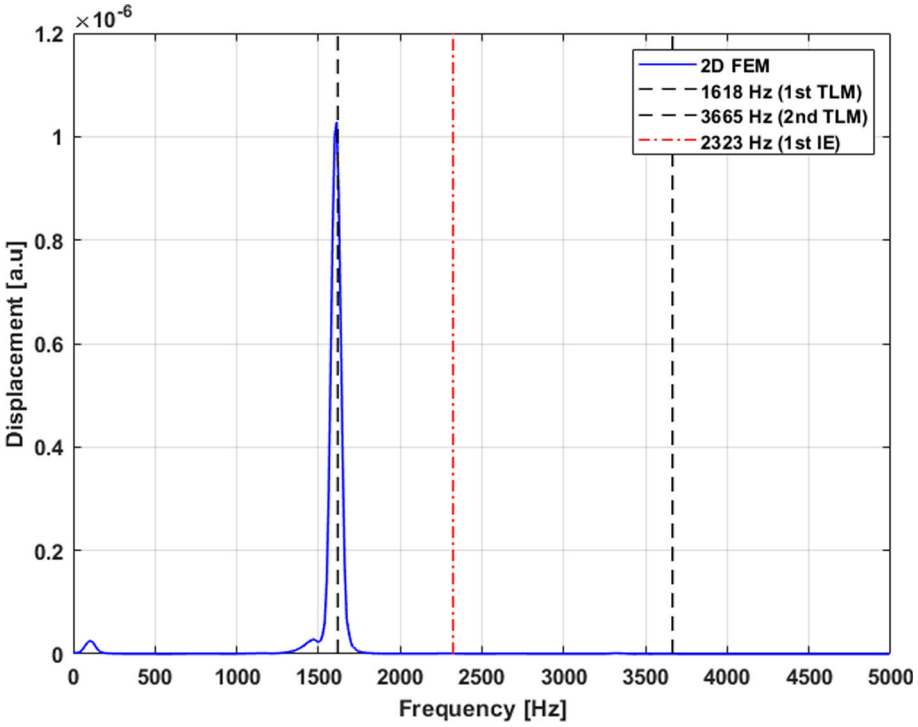

Figure 5. Peak simulated by 2D FEM simulation, the black striped lines indicate the resonances predicted by the TLM model and red striped is predicted by the impact-echo (IE) model.

peak predicted for the refractory-skull interface would be predicted to stay at the same frequency.

The TLM model rather predicts a shift of the main peak at 1618 to a lower frequency of 1206 Hz.

To test this hypothesis a layer of 20 cm thick skull is added to the model. For simplicity, an open boundary condition is applied. The result is shown in Figure 6. Notice that the second peak predicted by the TLM model at 2583 Hz is also present, however, it is slightly overestimated by the TLM model. The PRF is not able to predict the correct frequency. In this case, the liquid beyond the skull interface is still left out of the models. The effect of the presence of a skull and liquid and slag will be treated in the discussion.

For inversion not only the thickness of the semi-graphite layer is to be estimated, but also the thickness of the skull. Hence, a simple 1D inversion model based upon a single dominant frequency will no longer work in this case. This is an important insight that is provided by the TLM model.

In the Tata Steel blast furnaces, the lining geometry contains more layers. In this case, a 6 cm thick shell layers is followed by a layer of 40 cm safety graphite. The safety graphite is followed by a 4 cm thick ramming layer, and finally a thickness of 83 cm is chosen for the semi-graphite layer. The geometry is shown in (Figure 7).

According to the PRF model, the graphite-ramming and ramming-semigraphite interfaces will produce a frequency below 5 kHz at a fixed position.

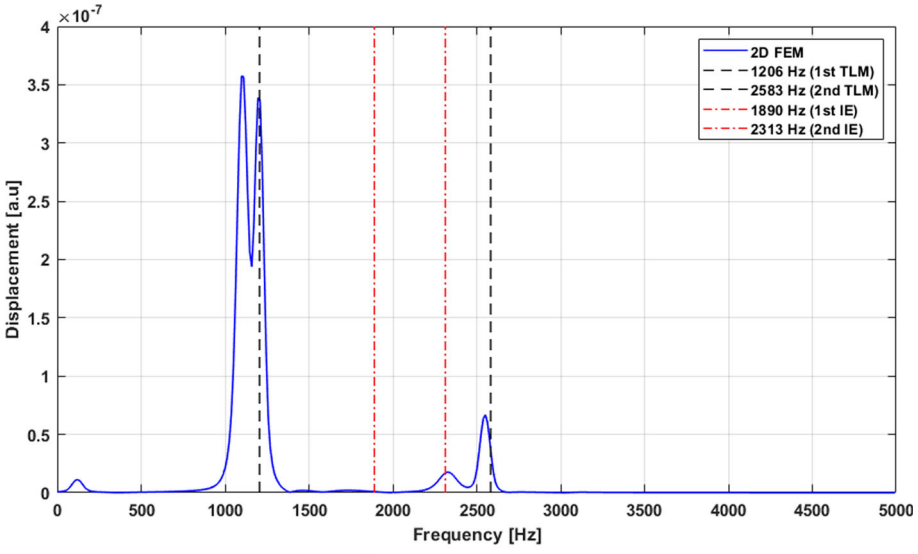

Figure 6. A 40 cm semi-graphite and 20 cm of skull.

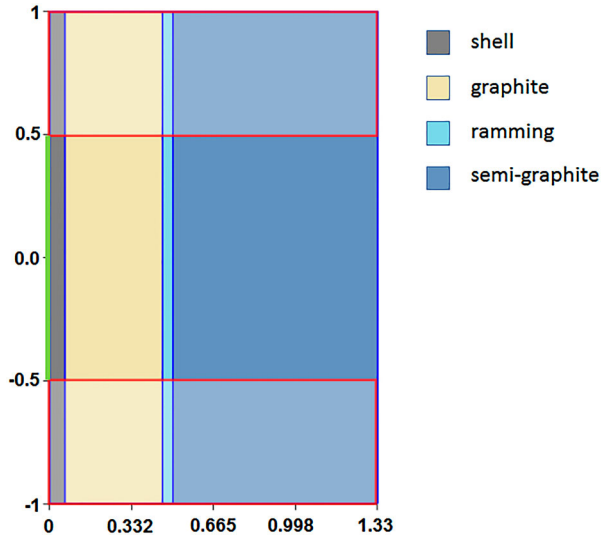

Figure 7. Schematic lining setup for the IJmuiden blast furnace.

Figure 8 shows the spectrum calculated by the 2D FEM method. In the same figure the results from the TLM and the PRF methods are visible. Looking at the first peak in the spectrum, a difference of 147 Hz is found. If we use the PRF formula in reverse, this comes down to 1.63 m, therefore a 33 cm difference.

In Figure 9, the wall erosion prediction curves are shown. For inversion, the lowest peak in the spectrum is chosen. A distance remains between the curves even when the refractory is very thick.

Application of the 1D models in case of more complex geometries

In the following, three simplified geometries of a blast furnace hearth are considered. The first case shows a furnace with an inclined erosion interface. Case 2 considers a furnace that has an erosion profile containing a so-called elephant's foot. In Case 3, a furnace is considered with a ramming layer that is further away from the shell, this situation is found in the Tata Steel blast furnaces.

Case 1: a slanted erosion line

The first geometry under consideration is shown in Figure 10. The red area represents the semi-graphite layer in the furnace and is given similar parameters. The green layer is an 8 cm thick ramming layer. The blue layer is the shell layer which is chosen to be 6 cm thick. The simulation is done using axisymmetry.

Several assumptions are made in the model. The materials have an ideal connection and the seams between the bricks are neglected. The dependence of the material properties on temperature is not considered here. The materials are considered isotropic.

Figure 11 shows the amplitude of the propagating wave after 0.86 ms where the wavefront reaches the internal boundary. This figure nicely illustrates the spherical wavefront that sweeps out a large part of the furnace wall. Therefore, the assumption that the wave will propagate in a straight line is not realistic. A strong wave is trapped in the shell layer. Notice that in practice, this wave will be reflected on the many thermocouples and irregularities on the shell. This will result in colored noise within the measurement.

For the test a source-receiver pair is placed at five different heights along the shell. For each height, a distance to the interface at the hot side of the furnace is measured. The distances are tabulated in Table 2. In the same table, the predicted frequencies are shown considering both 1D models.

The next step is the examination of the frequency spectrum produced at each height. This brings forward a difficult issue of how to select the frequency. In Figure 12, the resulting spectra are shown. The red crosses indicate the peaks expected by the TLM model, and in green, the peak position that is predicted by the PRF model. Except

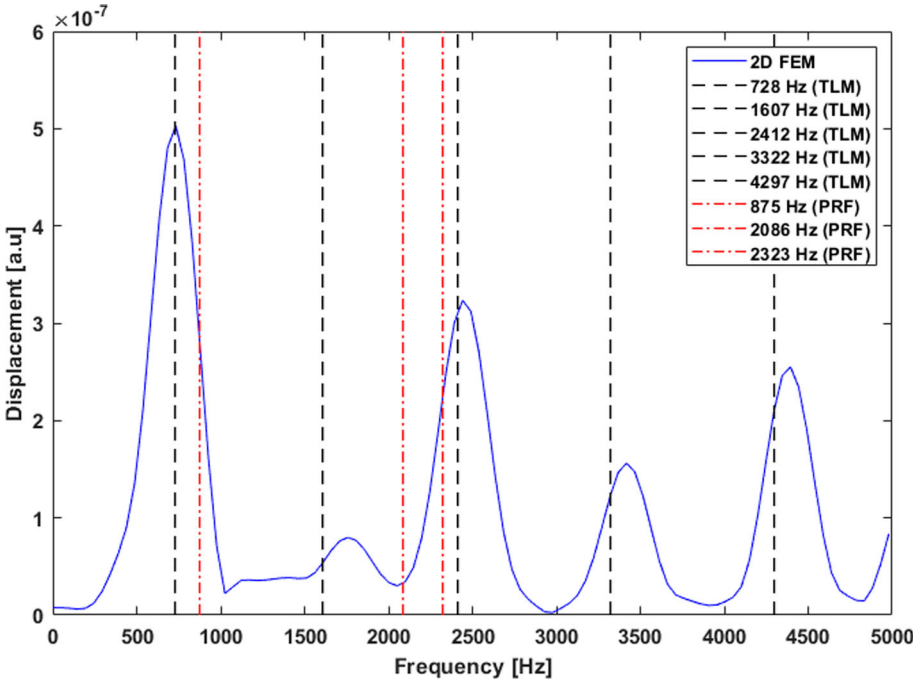

Figure 8. Spectrum calculated by 2D FEM and by the 1D transmission line method and by the impact-echo method.

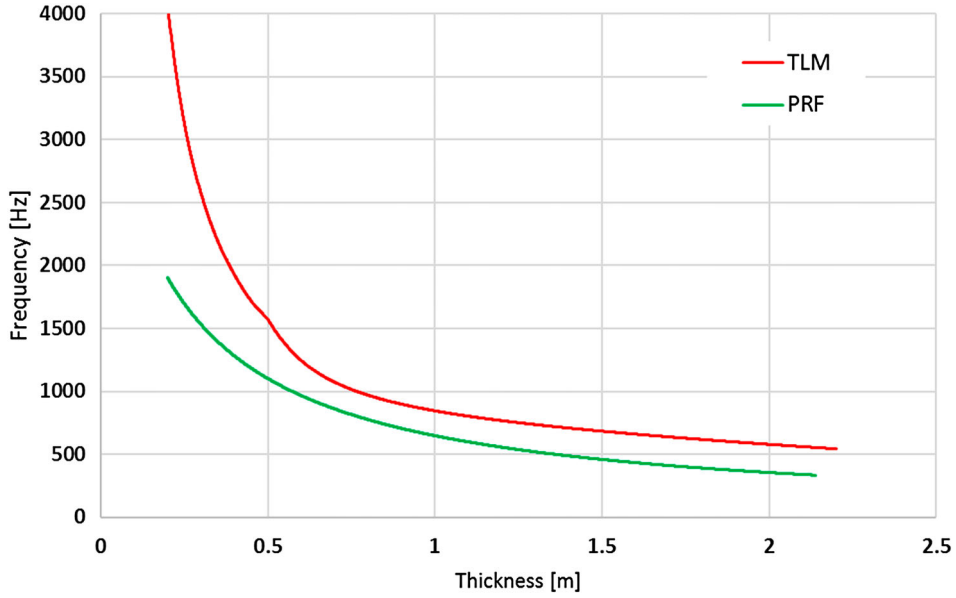

Figure 9. Prediction curves according to the TLM and the PRF method.

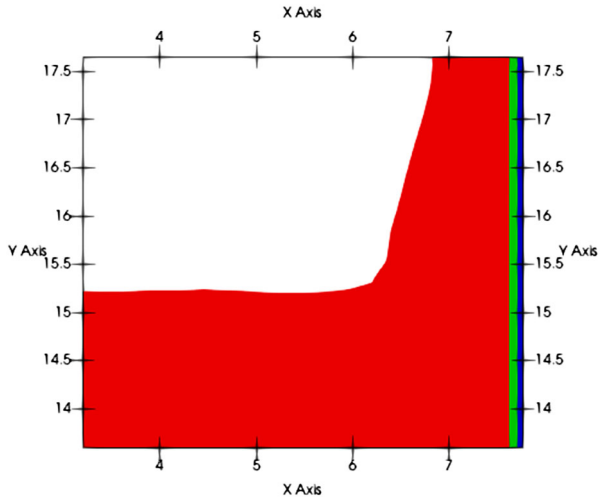

Figure 10. False color plot showing the different regions. Red: semi-graphite, green: ramming and blue: shell.

for the lowest height, the predictions are close to the peak at the lowest frequency ignoring the peak at around 500 Hz, which would predict a wall thickness larger than the uneroded thickness. A similar strategy is published in [8]. The lowest height poses a problem for this strategy, the measurement height is just below the bending point of the erosion line. At this height, a slight movement up and down would result in a large difference in the horizontal distance. Moving the measurement point somewhat lower would bring the height below the bottom of the erosion line. In this case, the lowest peak seems a better choice.

The selected 'dominant' frequency can be used to predict the remaining wall thickness. The resuling prediction errors are tabulated in Table 3, the results are presented graphically in Figure 14. In this case, the differences between the IE and TLM method are small. Large differences are found if the results are compared to the true distance. The difference is the smallest for the TLM method. The largest deviation of

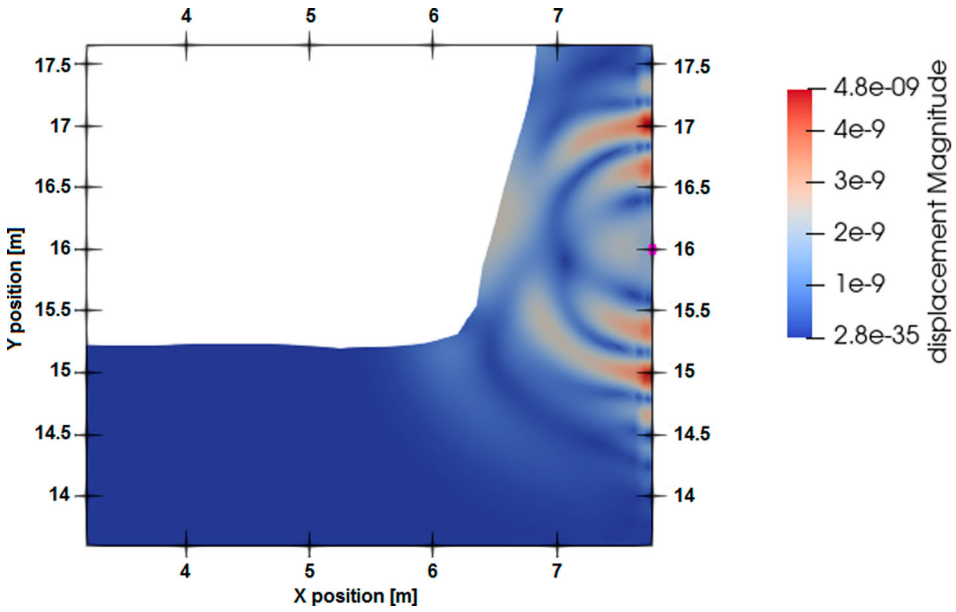

Figure 11. Plot of the wave amplitude 0.5 ms after the peak of the source pulse. The pulse takes about 0.5 ms to arrive at the hot face. The false color indicates the amplitude of the signal, clearly the pulse spreads out throughout the entire hearth wall at the point the peak reaches the hot face.

Table 2. Predicted frequencies and thicknesses against height.

Source height	Distance [m]	PRF [Hz]	First peak [Hz]	FEM frequency	Inverse PRF [m]	Inverse TLM [m]
15.2	2.55	502	505	732	1.74	1.71
15.6	1.41	903	862	781	1.63	1.59
16.0	1.33	957	904	745	1.71	1.68
16.4	1.22	1041	969	928	1.37	1.30
16.8	1.11	1143	1042	1050	1.21	1.10

Table 3. Resulting errors of the single peak inversion using the TLM and IE models.

Source height	Error PRF [m]	Error TLM [m]	Error PRF [%]	Error TLM [%]
15.2	−0.81	−0.84	−31.8	−32.9
15.6	0.22	0.18	15.6%	12.8
16.0	0.38	0.35	28.6	26.3
16.4	0.15	0.08	12.3	6.6
16.8	0.1	−0.01	9.0	−0.9

84 cm is found at the lowest height, however, in this case, the measurement is almost below the bottom of the liquid bath. Even if we neglect this result, the deviation at the height of 16 m is 35 cm, or 26% larger than the true thickness. One may argue that a peak at a higher frequency should have been selected. The peak at 1025 Hz, for example, would result in a wall thickness of 1.14 and, indeed, the difference will now be −19 cm, which is still an error of 14%. This is quite large considering that many problems that we encounter in the real world are still neglected. (Table 3).

Case 2: elephant's foot

Another test case is shown below. In this case a so-called elephant's foot is present. Again, the red is a semi-graphite area, the green area a ramming layer and blue is a shell layer as shown in Figure 14. The spectra which result from simulation are shown in Figure 15. The red crosses indicate the peak positions as predicted by the TLM model and the green cross is the prediction from the PRF model.

In Table 4, the results are summarized similar to the previous case. In Figure 16 the results from the two 1D models are represented by the two lines.

Now the strategy seems that picks the peak closest to the predicted peaks seems to pick the highest peak in the spectrum.

The errors, in this case, are summarized in Table 5. For the PRF method, the deviation is quite high; peaking at 42% overestimation of the wall thickness. The TLM model gives more reasonable results with a maximum of 13.7% overestimation.

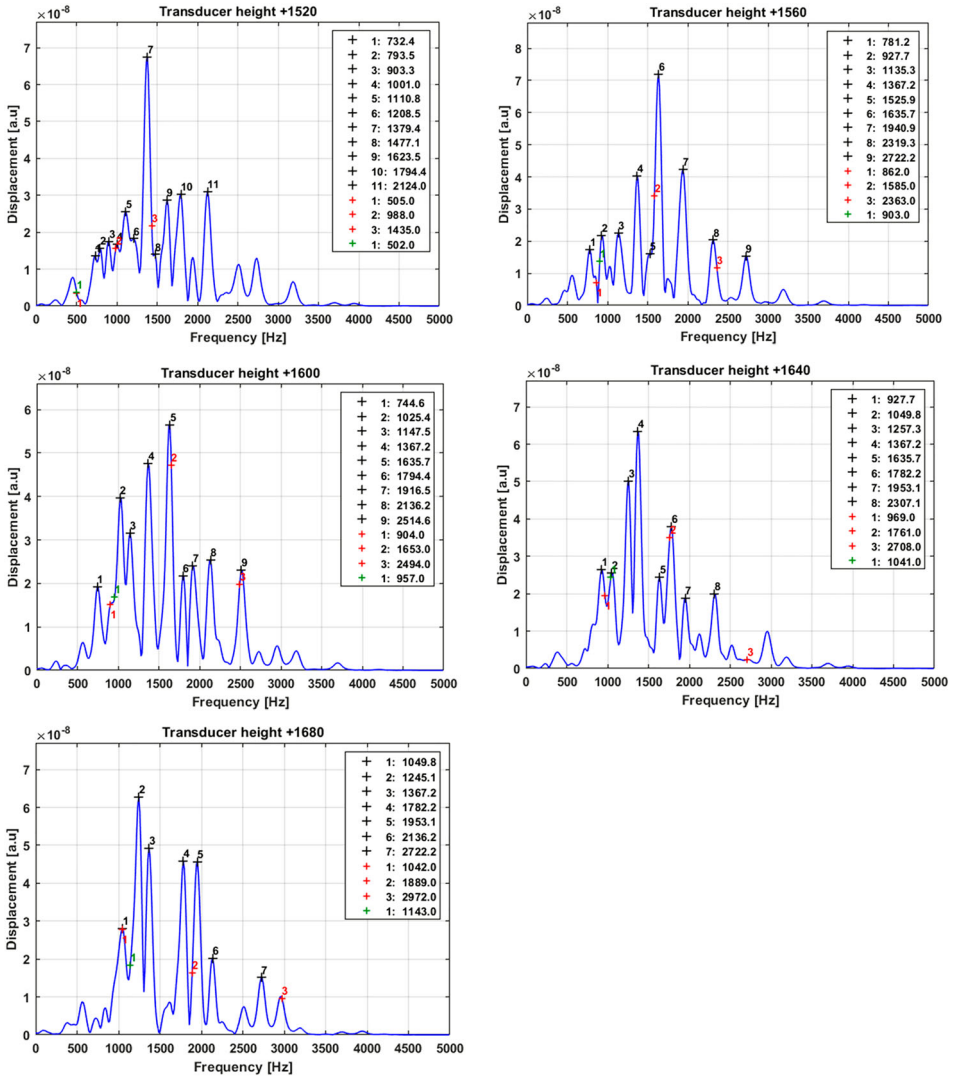

Figure 12. Spectra calculated for each measurement height for Case 1.

Table 4. Total thickness at the considered transducer heights.

Source height	Distance [m]	PRF [Hz]	First peak TLM [Hz]	FEM frequency	Inverse PRF [m]	Inverse TLM [m]
15.2	1.06	1196	1078	1148	1.105	0.973
15.6	0.70	1794	1263	1379	0.917	0.728
16.0	0.65	1928	1312	1367	0.925	0.739
16.4	0.78	1615	1191	1270	0.997	0.836
16.8	0.88	1435	1109	1233	1.028	0.875

Table 5. Resulting errors of the single peak inversion using the TLM and IE models.

Source height	Error PRF [m]	Error TLM [m]	Error PRF [%]	Error TLM [%]
15.2	0.045	−0.087	4.2	−8.2
15.6	0.217	0.028	31.0	4.0
16	0.275	0.089	42.3	13.7
16.4	0.217	0.056	27.8	7.2
16.8	0.148	−0.005	16.8	−0.6

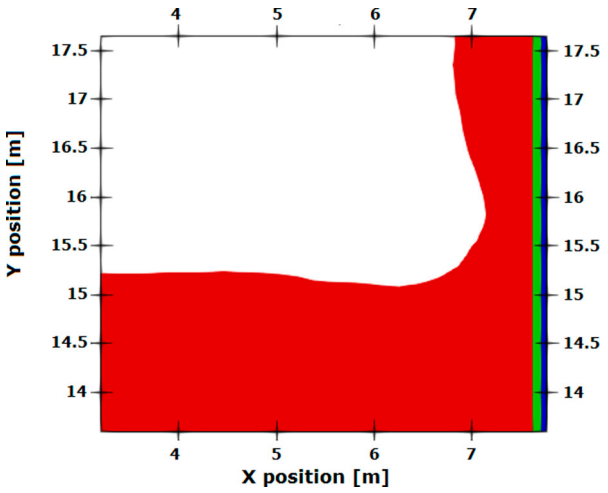

Figure 14. Geometry of Case 2 showing a common erosion pattern called elephant's foot. The shell has a blue colour the ramming layer a green colour and the red area is semi-graphite.

This largest error is close to the height of maximum erosion, so at the most critical position (Figures 13–16).

Case 3: ramming layer at distance from the shell

The blast furnaces in Tata Steel, IJmuiden, have a refractory setup that has a ramming layer that is 40 cm away from the shell. In Figure 17, the geometry setup is shown, in green there is a semi-graphite layer, light blue indicates a 4 cm thick ramming layer, purple indicates the 40 cm thick safety graphite layer and dark blue is the 6 cm thick shell. The yellow and red indicate two different types of bottom bricks. For simplicity, the yellow layer is given the same properties as graphite, and for the red region, the properties of semi-graphite are used. The goal is merely to see the influence of an additional interface at these points.

Table 6 contains the results for this case. In Figure 18, the predicted frequencies are plotted in the spectra resulting from the 2D FEM calculation shown in Figure 18.

From the spectra shown in Figure 18 it is found that picking the highest peak does not work here as the ramming layer will also produce a strong echo. There is no clear strategy that would make it possible to choose a dominant frequency to do the inversion on. Compared to the prediction of the TLM model for the 15.2 m height, the first peak would be closest, for 15.6 m, it is the second high peak in the spectrum that is close, while for 16 m height, it is close to the predicted position, for 16.4 m, the predicted location is in between the first two peaks.

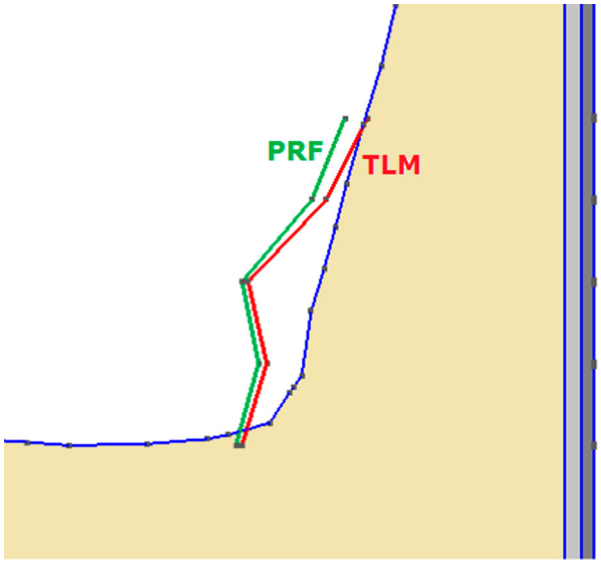

Figure 13. Results of the 1D inversion approach for the two methods for Case 1.

Discussion of results

The comparison of the 1D results with the 2D FEM results shows that both models are not matching very well. The approaches considered in these cases are still very theoretical and lack many real-world phenomena. In reality, the wave will propagate in a 3D space, which will mean that a part of the signal will be lost towards the sides, which may result in a lower signal-to-noise ratio, but also inhomogeneities in the sideway directions can scatter the wave back to the receiver.

Influence of the skull layer

In the simple square layer model for which the results were shown in Figure 5, it was found that the presence of a skull layer will significantly shift the peak with respect to the case where a soft acoustic medium is present. It is therefore important to know if the acoustic signal encounters a gas-filled crack in the refractory or if a well adherent skull is present.

The shift depends on the thickness of the skull layer and the acoustic impedance presented by the skull layer. This poses a difficult and fundamental problem that may limit the accuracy of the impact-echo method. It may be argued that in most blast furnaces, the bricks will be cracked, and the last interface that is measured is a gas-filled crack. This assumption also implies that it will be impossible to estimate the thickness of a skull layer. Even if there is a transmission of the acoustic skull layer, another difficulty is that the acoustic properties of the skull are not well known, and the composition of the skull may even vary over time. So even though the TLM is able to come up with reasonable estimates in the case of the skull layer, it would still suffer from the unknown material properties.

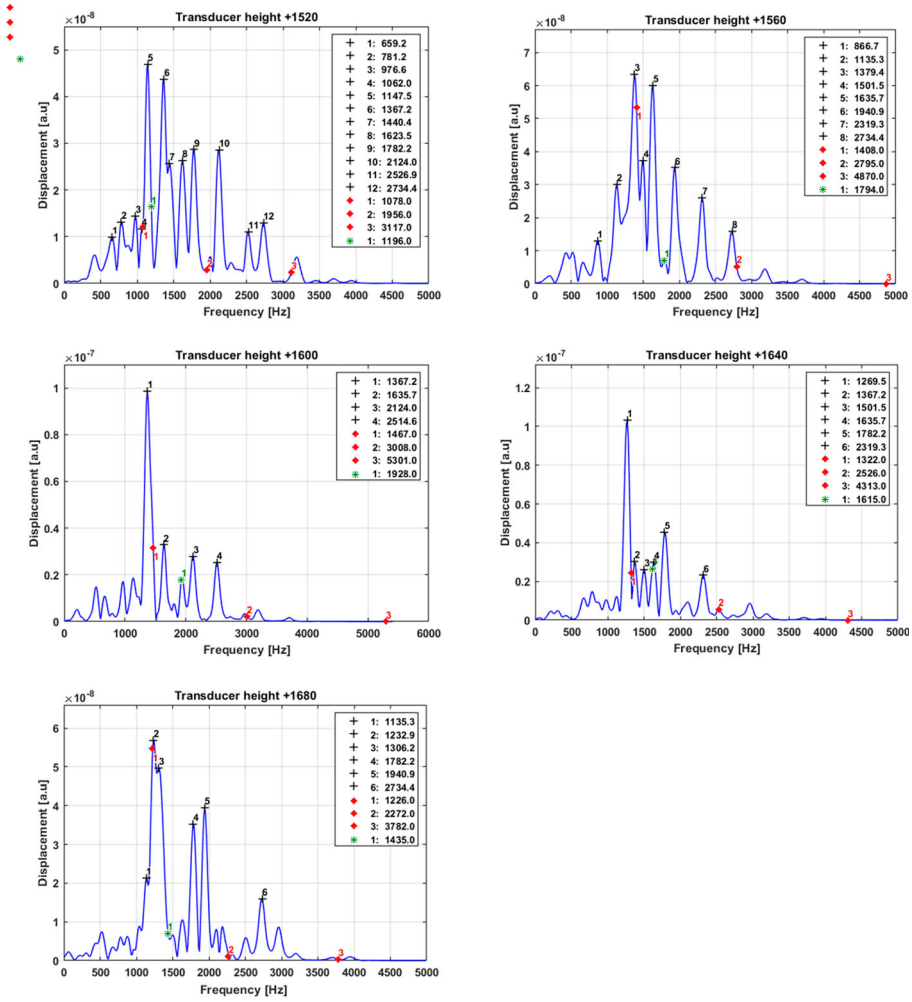

Figure 15. Spectra calculated for the different height in Case 2. The black crosses indicate the peaks calculated by the FEM model, the red crosses indicate the peaks predicted with the TLM model and the green cross is predicted by the PRF model.

In the spectra from the examples, it is clear that there are peaks in the spectrum which are below the peak that is chosen as the dominant peak. However, in the examples, no skull layer is present. In practice, one cannot be sure if the acoustic signal can reach the skull as the signal may be reflected of a large crack in the refractory. The peaks could, therefore, erroneously be interpreted as an indication of the presence of a skull layer.

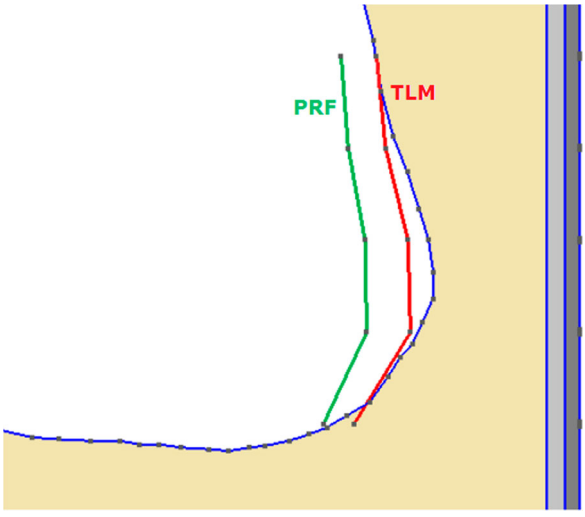

Figure 16. Profiles estimated by the 1D models, green for the impact-echo model and red for the TLM model.

Another issue is that the skull layer transits into the liquid iron, the difference in acoustic impedance of liquid and the skull will therefore be limited. A large portion of the energy transmitted into the skull layer will also be transmitted into the liquid. The skull-liquid interface is therefore expected to have a very weak reflection and most of the energy transmitted into the skull will be absorbed into the liquid iron. It is, therefore, unlikely that any acoustic method applied at the outside of the furnace will be able to predict the thickness of the skull layer.

In pure iron at the melting point the density drops from 7290 to 7017 kg m^{-3} and the sound velocity drops from 4730 to 3980 m s^{-1} [9]. If damping is neglected the acoustic impedance, Z, is equal to the multiplication of sound velocity and density. For an incoming wave at normal incidence on the interface, the amount of reflected wave pressure can be calculated using the reflection coefficient.

$$R = \left(\frac{Z_2 - Z_1}{Z_1 + Z_2}\right)$$

Filling in the numbers, we obtain a reflection coefficient of 0.105, the amplitude of the reflected pressure wave is 10.5% of the amplitude of the incoming wave. The intensity of the wave can be calculated by the square of the pressure divided by the impedance, only 1.1% of the incoming intensity is reflected towards the source. This means that 98.9% of the sound intensity will be transmitted into the liquid iron.

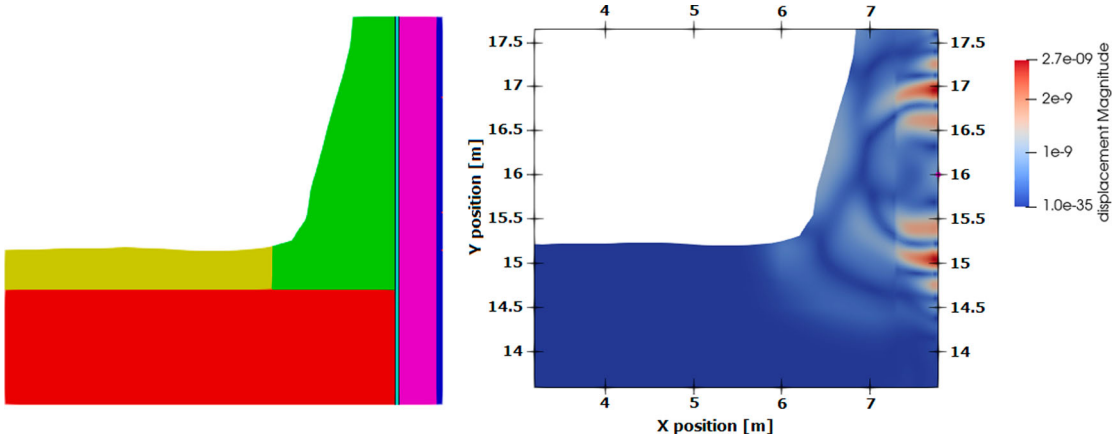

Figure 17. Left: geometry of Case 3. The dark blue layer represents the shell, the purple layer the safety graphite layer, in light blue the ramming layer, in green the semi-graphite layer and in yellow and red two different types of bottom bricks. Right: First arrival of the wave at the hot face about 0.55 ms after the peak of the pulse excitation.

Table 6. Summary of results from applying the impact-echo and TLM model to predict the 2D FEM outcomes.

Source height	Distance [m]	PRF [Hz]	TLM first peak [Hz]
15.2	2.55	479	428
15.6	1.41	830	706
16.0	1.33	875	728
16.4	1.22	946	761
16.8	1.11	1029	802

Using the transmission line method, it is possible to calculate the spectrum of the received signal in the case a skull layer is considered with free boundary condition and a case where an impedance boundary is applied which is equal to the case where all sound transmitted into the liquid iron is

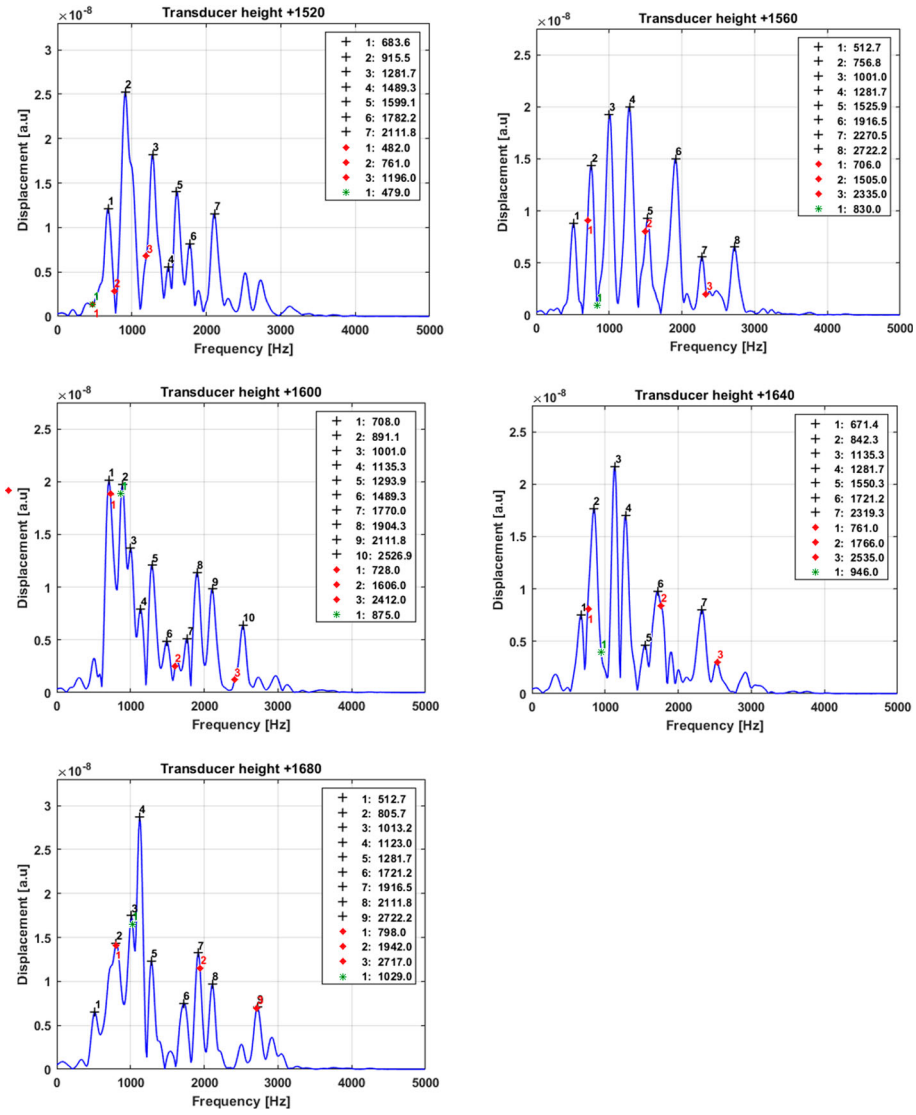

Figure 18. Simulated spectra for Case 3. The black crosses indicate the peaks calculated by the FEM model, the red crosses are resulting from the TLM model and the green cross is calculated with the PRF model.

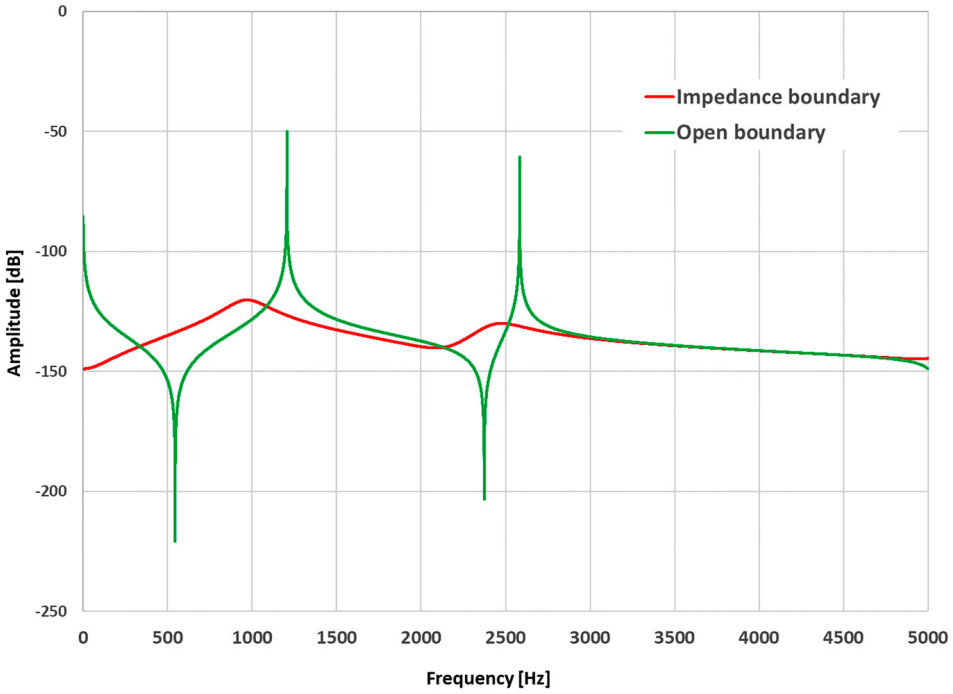

Figure 19. Spectrum calculated by the TLM method in case the skull has a free boundary condition (green) and an impedance boundary condition (red).

absorbed. The results of these calculations are shown in Figure 19.

In the case of an open boundary condition at the hot side of the skull 100% of the wave intensity is reflected, in the layers also, no damping is considered. This results in very narrow peaks in the spectrum. When an impedance boundary is considered, 98.9% of the wave intensity is absorbed. The peaks are now 70 dB lower and much broader and the peaks are shifted. The peak at 1206 Hz is now shifted downwards by 237 Hz. In Figure 20, the phase of the received signals is plotted. When an open boundary is applied, there are no losses accounted in the model. In this case, the phase will change 180 degrees at the resonance frequencies. When an impedance boundary is applied, the signal will be absorbed at the impedance boundary. In this case, the phase changes more gradually.

In reality, the skull layer is known to be inhomogeneous [10]. However, even when the density of the skull is varied from 1000 to 8000 kg m^{-3} or when the velocity in the skull is changed from 1000 to 8000 m s^{-1} the amplitude of the first peak varies between 123 and 120 dB and the frequency ranges from 575 to 988 Hz.

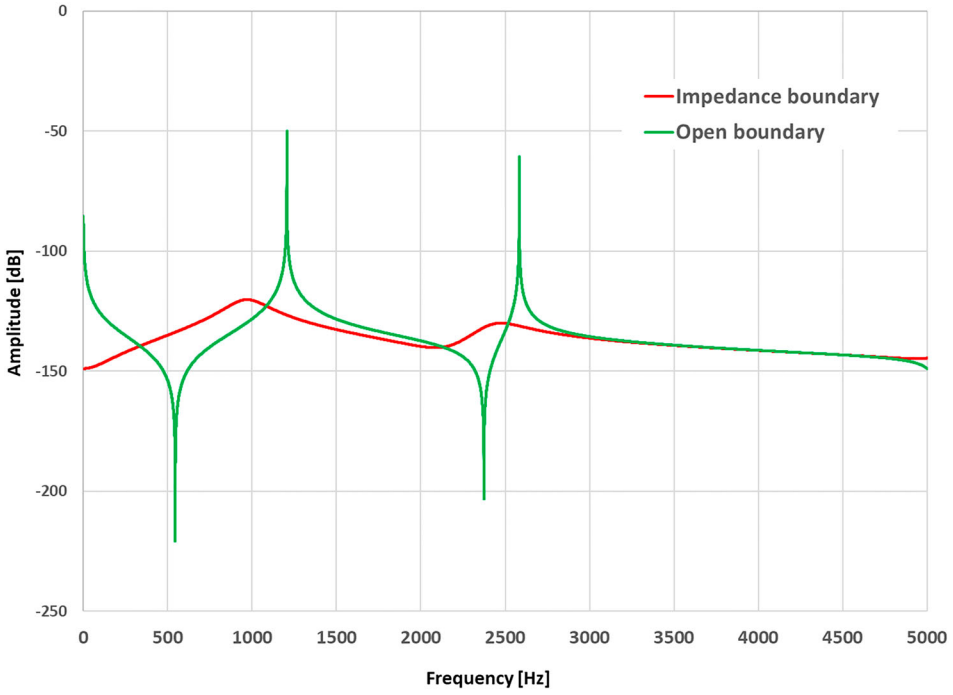

Figure 20. Phase of the received signal when an impedance boundary is assumed to simulate the sound being absorbed in the liquid iron, and in green the result for an open boundary condition.

Inverse temperature modelling

In Ref. [11], it is argued that thermal analysis of a blast furnace hearth wall suffers from discontinuities in the lining and changing material properties. However, any acoustic model would suffer from the same issues. Notice that a thermocouple pair can be inserted into the semi-graphite layer. Therefore, a thermocouple can extend beyond the ramming layer and the seam between the shell and the ramming, which the acoustic signal has to transit twice. Nowadays, it is possible to probe multiple depths at each thermocouple location. The thermocouples are always present, whereas the acoustic measurements are often samples in time. The big drawback of the thermocouples is their fixed position and the need to insert them into the furnace. It is interesting to make a comparison between the accuracies of the models considering these boundary conditions. The performance of a thermocouple inversion model will be heavily dependent on the implementation details, on the accuracy of the properties of the material and also on the amount of available thermocouples and the maintenance of the thermocouples themselves. Although a comparison may be made for a particular furnace, no general conclusions can be drawn from such effort. In Ref. [12], the result from an impact-method measurement based on the PRF method compensated for temperature effects is compared with the results from a thermal model, and initially, large deviations were found of about 29%. To solve this issue, the sound velocities were adapted to harmonize the results. This indicates that also in practical measurements, large corrections have to be applied when using the PRF method.

Conclusions and recommendations

In this paper, an alternative approach is presented to interpret the results of the impact-echo measurements on multi-layered structures using a 1D approach. The approach shows good results for a stack of flat layers when compared to a 2D FEM approach.

Simple layered models were chosen that have a simple structure, namely, a shell, a ramming layer and a refractory layer. This structure is found in some of the big blast furnaces worldwide [13]. The proposed model predicts the frequency within a few Hertz, while the impact-echo method can deviate by more than 100% for small wall thicknesses. In addition, the presence of a skull layer introduces an additional error in the impact-echo models. From these simple models, it can be seen that the presence of skull will shift the main peak that is associated with the thickness of the refractory. This can introduce large errors for both the TLM and the impact-echo model when a simple inversion method is used based upon the inversion using a single peak.

The traditional impact-echo predicts one peak per interface. The TLM method will not only predict the position of the peak related to the thickness mode, but also its harmonics. For further development of the models, it is possible to use this extra information such that better predictions in the presence of skull can be made.

The 1D models have been compared to the outcome of three cases solved using a 2D axisymmetric FEM simulation. In these cases, a vertical cross-section of the furnace hearth have been simulated. The first case being a furnace with a slanted wall on the hot side. The thickness of the wall was overestimated by about 26%, for the second case where an elephants' foot profile is considered. The largest error was found to be an overestimation of 14%. For the third case, a refractory concept such as used in Tata Steel, IJmuiden, was investigated. In these furnaces, a ramming layer is present away from the shell. In this case, no clear strategy is available for selecting the proper peaks used for a 1D single frequency inversion model.

The impact-echo suggests the selection of a dominant peak from the spectrum to predict the wall thickness. It is shown in this work that a strategy for picking this peak is not trivial even for the ideal cases that have been considered.

To be able to increase the accuracy of the models, it will be interesting to use a full-wave inversion approach in which the output of multiple transducers is combined in a 2D or even 3D calculation model.

Disclosure statement

No potential conflict of interest was reported by the author(s).

ORCID

Rudolf Sprik http://orcid.org/0000-0002-1573-1071
Chris Stolk http://orcid.org/0000-0002-0944-3428

References

[1] Sansalone MJ. Impact-Echo: The complete story. ACI Struct J. 1997; Vol.94(6):777–786.
[2] Sansalone MJ, Streett WB. Impact-echo: non-destructive evaluation of concrete and masonry. Jersey Shore: Bullbrier Press; 1997.
[3] Gibson A, Popovics JS. Lamb wave basis for impact-echo method analysis. J Eng Mech. April 2005; Vol. 131(4).
[4] Pollard HF. Resonant Behaviour of an Acoustical Transmission Line. Aust. J. Phys. Dec 1962; Vol. 15:p. 513.
[5] Pollard HF. Acoustic waveguides. In. Sound waves in solids. London: Pion Limited; 1977. p. 115.
[6] CSC – IT CENTER FOR SCIENCE LTD, *Elmer FEM*, 2020-11-11, Version 9.0.
[7] Sadri A, Ying W, Gebski P, et al. A comprehensive review of acousto ultrasonic-echo (AU-E) technique for furnace refractory line assessment. COM. 2015;2015.
[8] Wang C-Y, Chiu C-L, Tsai K-Y, et al. Inspecting the current thickness of a refractory wall inside an operational blast furnace using the impact echo method. NDT&E Int. 2014;66: 43–51.
[9] Wagle F, Steinle-Neuman G. Electrical resistivity discontinuity of iron along the melting curve. Geophys J Int May 2018; Vol. 213:237–243.
[10] Perepelitsyn VA, Zemlyanoi KG, Mironov KV, et al. Mineralogy and microstructure of skulls version in AO EVRAZ NTMK blast furnace No. 6. Refract Ind Ceram. Nov 2020; Vol. 61 (6)):364–373.
[11] Sadri A, Henstock M, Ying WL. Predicting blast furnace reling timing: methods, results, and comparisons. 5th ESTAD, Stockholm, 2021.
[12] Ma J, Wen X, Zhao X. Detection of blast furnace hearth lining erosion by multi-information fusion. IEEE Access. July 2021.
[13] K. Raipala, On hearth phenomena and Hot metal carbon content in the blast furnace [PhD Thesis]. Helsinki: Helsinki University of Technology; 2003.
[14] Gómez P, Fernández J, Ares A, et al. Reflections on the spectral peak in an impact-echo test by guided wave arguments. Berlin: NDT-CE; 2015.